Surface modified halloysite nanotubes reinforced polylactic acid for use in biodegradable coronary stents

Yuanyuan Chen[1], Alan Murphy[2], Dimitri Scholz[3], Luke M. Geever[4], John G. Lyons[5], Declan M. Devine[*]

[1, 2, 4, *] *Materials Research Institute, Athlone Institute of Technology, Ireland*

[5] *Applied Polymer Technology, Athlone Institute of Technology, Ireland*

[3] *Conway Institute, University College Dublin, Ireland*

Keywords: surface modification, 3-aminopropyltriethoxysilane, halloysite nanotubes, poly lactic acid, nanocomposites

Abstract:

Poly lactic acid (PLA) was reinforced halloysite nanotubes (HNTs) in this study. To improve dispersion and interfacial adhesion of HNTs within the PLA matrix, HNTs were surface modified with 3-aminopropyltriethoxysilane (ASP) prior to compounding with PLA. PLA/ASP-HNTs nanocomposites were characterised by differential scanning calorimetry (DSC), Fourier transfer infrared spectroscopy (FTIR), surface wettability, thermogravimetric analysis (TGA), transmission electron microscopy (TEM) and tensile testing. The hemocompatibility and cytocompatibility of PLA and PLA composites were investigated and the *in vitro* degradation process of PLA/ASP-HNTs composites was investigated for a period of 6 months by gel permeation chromatography (GPC), FTIR, weight loss measurement, DSC and tensile testing. **Results:** PLA and all PLA composites were blood compatibile and non-cytotoxic. TEM analysis revealed that HNTs agglomeration in PLA matrix was reduced by surface treatment with ASP. ASP-HNTs had better reinforcing effect than unmodified HNTs evidenced by tensile testing. ASP-HNTs appeared to increase the hydrolytic degradation process as measured by weight measurement. PLA/ASP-HNTs composites displayed 12.1% weight loss and 30.6% average molecular weight reduction while retaining 74% of Young's modulus by the 24th week of degradation. Based on this data, the reinforcement of PLA using ASP-HNTs may prove beneficial for applications such as biodegradable stents.

[*] Corresponding author. ddevine@ait.ie; Tel.: +353 90 6424553; fax: +353 90 6424493
[1] Email: ychen@research.ait.ie
[2] Email: amurphy@ait.ie
[3] Email: Dimitri.scholz@ucd.ie
[4] Email: lgeever@ait.ie
[5] Email: slyons@ait.ie

1. Introduction

Polylactic acid (PLA) is one of the strongest polymers in the biodegradable polymer category, and it has excellent biodegradability and good biocompatibility [1]. It has a long history in medical applications, such as biodegradable sutures in the repair of the Achilles tendon (e.g. Bio-Anchor, Bio-PushLock) [2,3], bone fixation devices (e.g. SmartNail, SmartScrew) [3,4], anti-adhesive tissue barriers (e.g. SurgiWrap®, REPEL-CV®) [5]. Poly L-lactic acid (PLLA), a type of PLA that only contains L-lactic acid, has been used for fully biodegradable coronary stents (e.g. Absorb BVS).

Fully biodegradable coronary stents, which provide transient vessel support with drug delivery capability, and degrade away after service without the long-term limitation of metallic stents, appear to be an ideal option to treat coronary heart disease. Currently, at least 28 companies are developing fully biodegradable stents [6]. Absorb biodegradable vascular scaffold (BVS) from Abbott has been approved by US Food and Drug Administration (FDA), and becomes the first commercially available biodegradable coronary stent in USA [7]. However, a very recent investigation of Absorb BVS among cardiologists conducted by cardiovascular research foundation (CRF) revealed that the thick strut of Absorb BVS may increase the risk of scaffold thrombosis [8]. Compared to metallic stents, polymeric stents tend to have thicker strut to withstand the minimal pressure from the artery wall of 300mmHg [9]. Absorb BVS has a strut thickness of 150 μm [7], while Synergy which is made from Platinum Chromium Alloy has a strut thickness of 74 μm [10]. The strut thickness directly links to stent performance and restenosis rate [11].

To achieve a thinner stent strut, a reinforced biodegradable polymer composite is a potential solution. PLA and high-aspect-ratio halloysite nanotubes (HNTs) were melt blended in our previous study, and it was found that HNTs significantly increased stiffness and Young's modulus of PLA. However, morphological analysis carried out using SEM indicated that complete intercalation did not occur as large microrange particles were clearly visible in the photomicrograph. Additionally, the void content in the composites increased with increasing HNTs content and gaps were observed between PLA and HNTs by SEM [12].

A desirable interfacial affinity between HNTs and PLA is a crucial factor for enhanced performance of PLA/HNTs nanocomposites. HNTs have certain advantages over plate clays such as montmorillonite, hectorite and saponite, which are strongly stacked to each other, but HNTs still remain difficult to achieve a good dispersion in the polymer matrix and tend to form micro-sized aggregates [13]. It is also reported that the relatively low content of hydroxyl groups on the surfaces of HNTs makes it easily to be dispersed in non-polar polymers using shear force due to the interactions between the HNTs and the polymer backbone, but this natural hydrophobicity of HNTs is not sufficient for interfacial adhesion in composite systems [14]. Hence, various surface treatment and modification of HNTs have been investigated. Prashantha *et al*. investigated unmodified HNTs and quaternary ammonium salt treated (QM-HNTs) compounded with polypropylene, and found that a better dispersion in the case of QM-HNTs compared to unmodified HNTs [15]. Haroosh *et al*. also reported that a better dispersion was obtained in the case of 3-aminopropyltriethoxysilane modified HNTs compared to unmodified HNTs in compounding with PLA/Polycaprolactone [16]. Deng *et al*. modified HNTs with potassium acetate and reported improved mechanical properties in HNTs/epoxy composite [17].

In this current study, 3-aminopropyltriethoxysilane (ASP or APTES) with chemical structure of $H_2N(CH_2)_3Si(OCH_2CH_3)_3$ was used to reduce the surface hydroxyl group content on the surface of HNTs. The amino groups of ASP was introduced to HNTs by grafting ASP in Al-OH bond in the internal lumen surface of HNTs forming covalent Al-O-Si bonds between ASP

and HNTs [14,18], and PLA interacted with siloxane groups of HNTs via hydrogen bonding [19]. ASP modified HNTs can promote good adhesion by improving the degree of crosslinking in the interface region and offer a suitable bonding between HNTs and PLA. ASP is a silane coupling agent and often used as intermediate to bond organic polymers to inorganic materials, such as fillers, glass, by adding amino groups, which can crosslink and immobilise molecules [18]. ASP treated glass surface has been reported to be superior to untreated glass surface for coating with extracellular matrix protein when used as a cell culture substrate to observe cell physiology and behaviour [20]. The effect of ASP modified HNTs on PLA/ASP-HNTs composites was investigated via tensile testing, differential scanning calorimetry (DSC), fourier transfer infrared spectroscopy (FTIR), thermogravimetric analysis (TGA) and transmision electron microscopy (TEM). In addition, blood compatibility and cytotoxicity of PLA and PLA composites were studied according to ISO-10993 and ASTM standard 756 through hemolysis test and MTT assay [21–23]. Finally, a period of 24 weeks *In vitro* degradation of PLA/ASP-HNTs composites was carried out in this study.

2. Materials and methods

2.1 Materials

PLA was obtained from NatureWorks LLC in US, Ingeo biopolymer 7032D. Halloysite nanotube (HNTs) was supplied by Applied Minerals in US, DRAGONITE-HP. 3-aminopropyltriethoxysilane was received from TCI chemicals in Japan. Chloroform and methanol were purchased from Sigma-Aldrich in US. All materials were used as received.

2.2 HNTs modifications

The grafting of ASP onto HNTs is illustrated in figure1, ASP was joined to the surface hydroxyl groups of HNTs [16,24,25]. Firstly, 300ml chloroform and 150ml methanol was mixed to form 450ml solvent solution in a fume hood, and 30ml ASP was added to this solution. Secondly, 30g HNTs were added to the solution and ultra-sonicated for an hour at room temperature. Then the mixture was put on the hot plate at 120°C, 1000 rpm stirring for 6 hours to form chemical bonding between HNTs and ASP. Thereafter, HNTs were filtered and washed twice with chloroform/methanol solution to remove the untreated HNTs, and the resultant ASP treated HNTs were left to dry for 3 days to let the solution evaporate completely. Finally, ASP treated HNTs were milled down by Retsch ball mill.

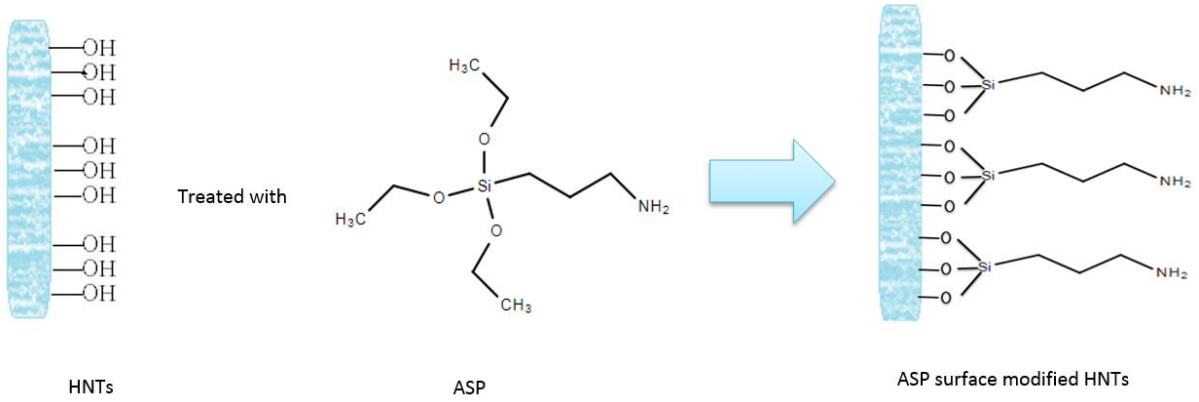

Figure 1: Sketch of ASP modification mechanism and interaction between HNTs and PLA.

2.3 Blends compounding

Composite films of PLA, PLA/HNTs 1wt%, PLA/HNTs 2wt%, PLA/HNTs 5wt%, PLA/ASP-HNTs 1wt%, PLA/ASP-HNTs 2wt% and PLA/ASP-HNTs 5wt% were prepared with mass fractions of 0, 1, 2, and 5wt% of HNTs and 1, 2, and 5wt% of ASP-HNTs respectively in the

PLA matrix. The thickness of all the films was below 1mm. All the composites were melt compounded using an a MP 19 TC 25 laboratory scale co-rotating twin-screw extruder (APV Baker, Newcastle-under-Lyme, UK) having 16 mm diameter screws and a length-diameter ratio L/D of 25/1, at temperature profile of 170/190/180/170/160/110/50°C, with a screw speed of 35 rpm, followed by 3 roll calendar system to form films. Prior to compounding PLA was dried at 80°C for 4 hours, HNTs and ASP-HNTs were dried at 100°C for 3 hours.

2.4 Differential scanning calorimetry

Differential scanning calorimetry (DSC) was carried out using a DSC 2920 Modulated DSC (TA Instruments) with a nitrogen flow rate of 20 ml/min to prevent oxidation. Calibration of the instrument was performed using indium as standard. All the samples were dried at 60 °C for 8 hours prior to testing. Test specimens weighed between 8 and 12 mg were measured on a Sartorius scales (MC 210 P), capable of being read to five decimal places. Samples were crimped in non-perforated aluminium pans, with an empty crimped aluminium pan used as the reference. The thermal history was removed by heating samples from 20 °C to 220 °C at the rate of 30 °C/min, and then held isothermally at 220 °C for 10 min. The samples were then cooled down from 220 °C to 20 °C at 30 °C/min. Finally, the thermal properties of the samples were recorded by heating the samples from 20 °C to 220 °C at the rate of 10 °C/min. Crystallinity, glass transition temperature and melting temperature of each batch were analysed. The percentage crystallinity of PLA in the composites can be calculated:

$$X_C = \frac{\Delta H_f}{\Delta H_f^{\circ} \times W} \times 100\%$$

Where, ΔH_f is the apparent melt enthalpy of the test samples, ΔH_f° is the melt enthalpy of completely crystalline PLA, which is 93.6 J/g [26], W is the weight fraction of PLA in the composites.

2.5 Fourier transfer infrared spectroscopy

Attenuated total reflectance Fourier transform infrared spectroscopy (FTIR) was carried out on a Perkin Elmer Spectrum One fitted with a universal ATR sampling accessory. All data were recorded at 21 °C in the spectral range of 4000–520 cm^{-1} against air as background, utilising a 4 scan per sample cycle at a resolution of 0.5 cm^{-1} and a fixed universal compression force of 70-80 N. Subsequent analysis was carried out using Spectrum software.

2.6 Morphology

Transmission electron microscopy (TEM Tecnai G^2 12 BioTWIN, FEI) was utilized to investigate the dispersion of ASP treated HNTs in PLA matrix and the morphologies of ASP treated HNTs. PLA/ASP-HNTs 5wt% composite film was embedded in monomeric EPON resin at room temperature, followed by polymerization at 60°C for 1 day. Subsequently, the cured EPON resin within PLA/ASP-HNTs 5wt% composite was cut into 80nm thick sections by using a Leica EM UC6 ultramicrotome. These sections were collected on 200 mesh thin bar copper grids. The TEM specimen was imaged using an acceleration voltage of 120KV.

2.7 Surface wettability

The surface wettability of the composites was assessed using a First ten angstroms, FTA32 goniometer. In this test the Sessile Drop contact angle technique was utilised with distilled water as the probe liquid. Five contact angle readings were recorded for each sample.

2.8 Thermogravimetric analysis

Thermogravimetric analysis (TGA) was performed to evaluate the thermal stability of PLA/ASP-HNTs composites. Tests were conducted using Perkin Elmer TGA 7

Thermogravimetric Analyzer, coupled with a Perkin Elmer Thermal Analysis controller TAC7/DX under nitrogen atmosphere. The tests were run from 30 °C to 600 °C, at a heating rate of 10 °C/min.

2.9 Mechanical testing

The mechanical properties of PLA and PLA composites were characterised by tensile tests. Standard tensile test specimens were prepared using a physical punching process on the melt blended film (ASTM D 638-03). PLA/HNTs composites were investigated previously in our study, but for comparative purposes both PLA/HNTs and PLA/ASP-HNTs composites were produced under the same condition in this current study. Tensile testing was carried out on a Lloyd Lr10k tensometer using a 2.5 kN load cell on ASTM standard test specimens at a strain rate of 50 mm/min. Data was recorded using Nexygen^{TM} software. The tensile tests were carried out in adherence to ASTM D 882. Five individual test specimens were analysed per group and prior to testing the thickness of each sample was measured. The percentage strain at maximum load, stress at maximum load, stiffness and Young's Modulus of each sample were recorded. Five replicates were carried out.

2.10 Hemolysis

The hemolytic properties of PLA, PLA/HNTs 1, 2, 5wt% and PLA/ASP-HNTs 1, 2, 5wt% were investigated by hemolysis test. Each polymer test sample was cut into a rectangular shape with 30cm^2 surface area as specified by ASTM standard [23] and sterilized with 70% isopropyl alcohol (IPA) and sterile phosphate-buffered saline (PBS). Subsequently, each sample was immersed in a 15ml falcon tube with 10ml sterile PBS. A positive control with 10ml deionized water and a negative control with 10ml sterile PBS were also prepared in 15ml falcon tubes. All the tubes were incubated for 30 minutes. Sheep blood in Alsever's solution (Cruinn diagnostics, Ireland) was centrifuged at 800 g for 10 minutes and washed with sterile PBS for 3 times to remove Alsever's solution. After removing the supernatant, the remaining red blood cells were diluted with sterile PBS to make 45% cell solution and further diluted with sterile PBS in a ratio of 4:5. Finally, 0.2ml of the diluted blood cell solution was added into each tube and incubated for 1 hour. Then all the tubes were centrifuged at 800 g for 10 minutes. Supernatant of each tube was collected in a 96 well plate and the absorbance was read at 545nm by plate reader (Synergy^{TM} HT BioTek plate reader). The hemolysis rate was calculated based on the average of 8 replicates:

$$\text{Hemolysis rate} = \frac{Asample - Anegative}{Apositive - Anegative}$$

2.11 Extract contact cell viability test - MTT assay

Human endothelial cells (HUVEC ATCC® CRL-1730) were used to assess the cells response to PLA composites. HUVECs were used at passage number of 13. The cells were cultured in F-12K medium (Kaighn's modification of Ham's F-12 medium, ATCC® 30-2004^{TM}), 10% fetal bovine serum (FBS), 0.1 mg/ml heparin, and 60 µg/ml endothelial cell growth supplement at 37°C in a humidified atmosphere of 5% CO_2. Medium was changed every second day.

The polymer specimens of PLA, PLA/HNTs 1, 2, 5wt% and PLA/ASP-HNTs 1, 2, 5wt% were prepared with 30cm^2 surface area as specified by ASTM standard [23], sterilized with 70% IPA and sterile PBS, followed by incubation in separate falcon tubes containing 10ml medium for 24 hours. The extract was used for cytotoxicity tests.

The cytotoxicity tests were carried out by extract contact. HUVECs were seeded into 96 well plates at a density of 1×10^4 cells/well and incubated for 24 hours to allow cells to attach. 100 µl extract from each falcon tube was then replaced in test wells. 100 µl fresh medium was placed in negative control wells and 100 µl 10% Triton X100 was placed in positive control

wells. The plates were incubated for 2 days and 6 days respectively. 100 µl of 10% MTT (3-(4,5-Dimethyl-2-thiazolyl)-2,5-diphenyl-2H-tetrazolium bromide) in medium was replaced in each well, followed by incubation for 3.5 hours. Subsequently, the MTT solution was removed and 100µl dimethyl sulfoxide (DMSO) was added to each well. The absorbance at 570nm was measured by plate reader (Synergy^{TM} HT BioTek plate reader). The percentage of viability can be calculated based on the mean of 5 replicates:

$$\text{Viability \%} = \frac{Asample}{Anegative}$$

2.12 In vitro degradation studies

The 2wt% loading of HNTs and ASP-HNTs in PLA matrix was chosen based on the observed reinforcing effect and unchanged T_g, indicating consistent stiffness of polymer chains. Ideally biodegradable stents should have adequate radial support for a period of 3 – 6 months to limit recoil and constrictive remodelling, and between 6 months and 5 years after angioplasty luminal enlargement takes place, as such the stents are only required for the first 6 months. Therefore, the *in vitro* degradation studies were conducted for 6 months in this study. PLA, PLA/HNTs 2wt% and PLA/ASP-HNTs 2wt% samples were immersed in falcon tubes containing 50 ml stimulated body fluid (SBF) and kept in water bath at 37 °C to mimic human body environment. The samples were weighed and collected at weeks 1, 2, 4, 9, 12, 16, 20 and 24. Characterisation of the samples were performed using DSC, FTIR, tensile testing and gel permeation chromatography (GPC). The test conditions of DSC, FTIR and tensile testing were the same stated above. The weight loss ratio was calculated by the formula below:

$$m_{loss} = \frac{(m_o - m_d)}{m_o} \times 100$$

Where, m_o refers to original mass and m_d refers to mass after degradation

2.11 Gel permeation chromatography (GPC)

A polymer laboratories (PL) GPC 120 was utilised to analyse the molecular weight of each sample. The system was fitted with two Agilent PL gel Mixed B 10 um columns using a 200 ul injection loop. The system was held isothermally at 40 °C for the duration of the test. The samples were dissolved (0.05% w/v) in tetrahydrofuran (THF). THF was used as the mobile phase with a flow rate of 1ml per minute.

2.12 Statistical analysis

Statistical analysis of PLA and PLA composites was performed using one way analysis of variance (ANOVA) with a Tukey Post hoc test to determine differences between specific halloysite loadings. Differences were considered significant when $p \leq 0.05$. The software used to perform statistical analysis was SPSS (IBM Version 22) for Windows. All data collected in this study were expressed as mean ± standard deviation. Sample size of 10 was used for tensile test and hemolysis test, 5 for contact angle test, 3 for cell viability test.

3. Results

3.1 Melt compounding

PLA/HNTs and PLA/ASP-HNTs composites were processed without difficulty. The extrudate changed in colour from transparent for virgin PLA to opaque with the inclusion ASP-HNTs.

3.2 Differential scanning calorimetry

DSC was carried out to investigate the thermal characteristics of PLA/ASP-HNTs composites and the results were recorded in table 1. The glass transition temperature (T_g) of PLA and

PLA/ASP-HNTs composites remained between 64 and 69°C, while the melting temperature (T_m) ranged between 172 and 174 °C. The cold crystallization temperature (T_{cc}) reduced slightly from 114.23 °C for virgin PLA to 108.48 °C for 1wt% ASP-HNTs/PLA composites and ~112 °C for 2 and 5wt% ASP-HNTs/PLA composites. The degree of crystallinity of PLA increased with the addition of ASP-HNTs from 37.46% for virgin PLA to ~39% for both PLA/ASP-HNTs 1wt% and PLA/ASP-HNTs 2wt% composites and 40.72% for PLA/ASP-HNTs 5wt% composites.

Table 1: Thermal analysis data for PLA/ASP-HNTs composites.

Samples	Glass transition temperature (°C)	Cold crystalline melting temperature (°C)	Melting temperature (°C)	Crystallinity %
Virgin PLA	66.6	114.23	173.61	37.46
PLA/ASP-HNTs 1wt%	64.3	108.48	173.89	39.38
PLA/ASP-HNTs 2wt%	64.3	112.12	172.6	39.14
PLA/ASP-HNTs 5wt%	69.07	112.68	172.82	40.72

3.3 Fourier transfer infrared spectroscopy

The chemical reaction of ASP modified HNTs and PLA/ASP-HNTs composites were analysed using FTIR. The spectrum of unmodified HNTs exhibited peaks at 3693 cm^{-1} and 3623 cm^{-1}, which were due to the O-H group vibration [16,27]. The peaks at 1119 cm^{-1} and 1000 cm^{-1} were because of Si-O stretching, and the peaks at 906 cm^{-1} was attributed to Al-OH groups [12,16,27]. However, when HNTs was treated with ASP, apart from the peaks mentioned new peaks appeared, such as O-H stretching at 3186 cm^{-1} , C-H stretching at 2980 cm^{-1} due to propyl chain of added ASP, N-H deformation at 1630 cm^{-1} and 1553 cm^{-1} signifying the grafting of ASP over the surface of HNTs [24], and deformation C-H bend at 1296 cm^{-1} [16]. Moreover, the perpendicular Si-O stretching at 1119 cm^{-1} was widened, and the intensity of Si-O bonding at 790 cm^{-1} and 750 cm^{-1} increased [16], shown in figure 2 A. The characteristic peaks of PLA located at 2995 cm^{-1} and 2946.34 cm^{-1} which are attributed to C-H stretch, and 1750 cm^{-1} connecting with stretching of the –C=O carbonyl group, shown in figure 2B [28]. When PLA was blended with the ASP modified HNTs, the peaks at 2996 cm^{-1} and 2945 cm^{-1} shifted and new peaks appeared at 2924 cm^{-1} and 2853 cm^{-1} (Figure 2 C).

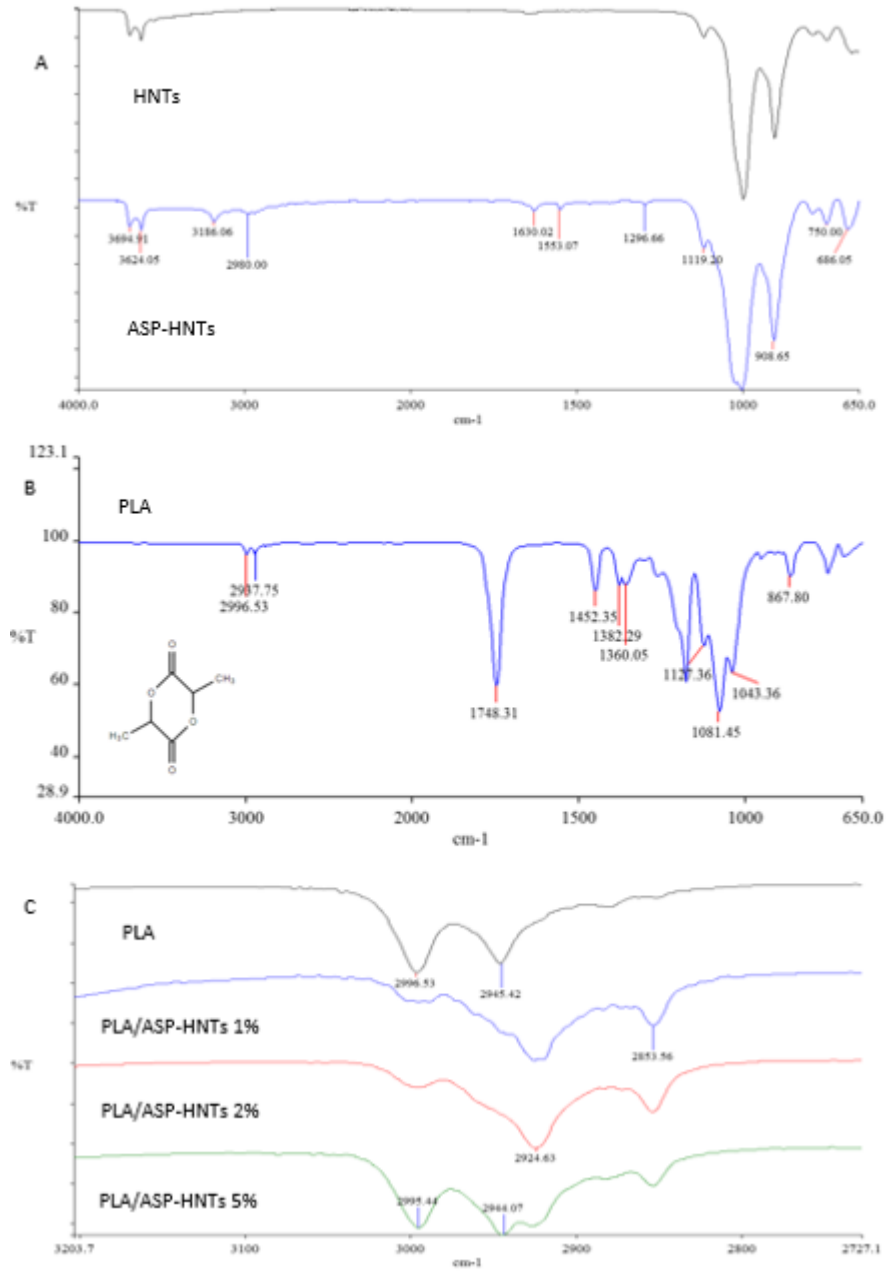

Figure 2: FTIR spectra of HNTs, ASP modified HNTs and PLA/ASP-HNTs composites A: HNTs and ASP modified HNTs. B: PLA. C: PLA/ASP-HNTs composites

3.4 Morphology

To observe the dispersion of ASP modified HNTs in PLA matrix, TEM was carried out on the PLA/ASP-HNTs 5wt% composite samples. It can be clearly seen that ASP modified HNTs, shown as dark particles, dispersed well within PLA matrix in figure 3. HNTs displayed a tubular shape and the diameter was visible in figure 3. The tubular shape of the HNTs is due to the misfit of the octahedral gibbsite-like sheet and the siloxane sheets [17]. Some small ASP-HNTs clusters were visible.

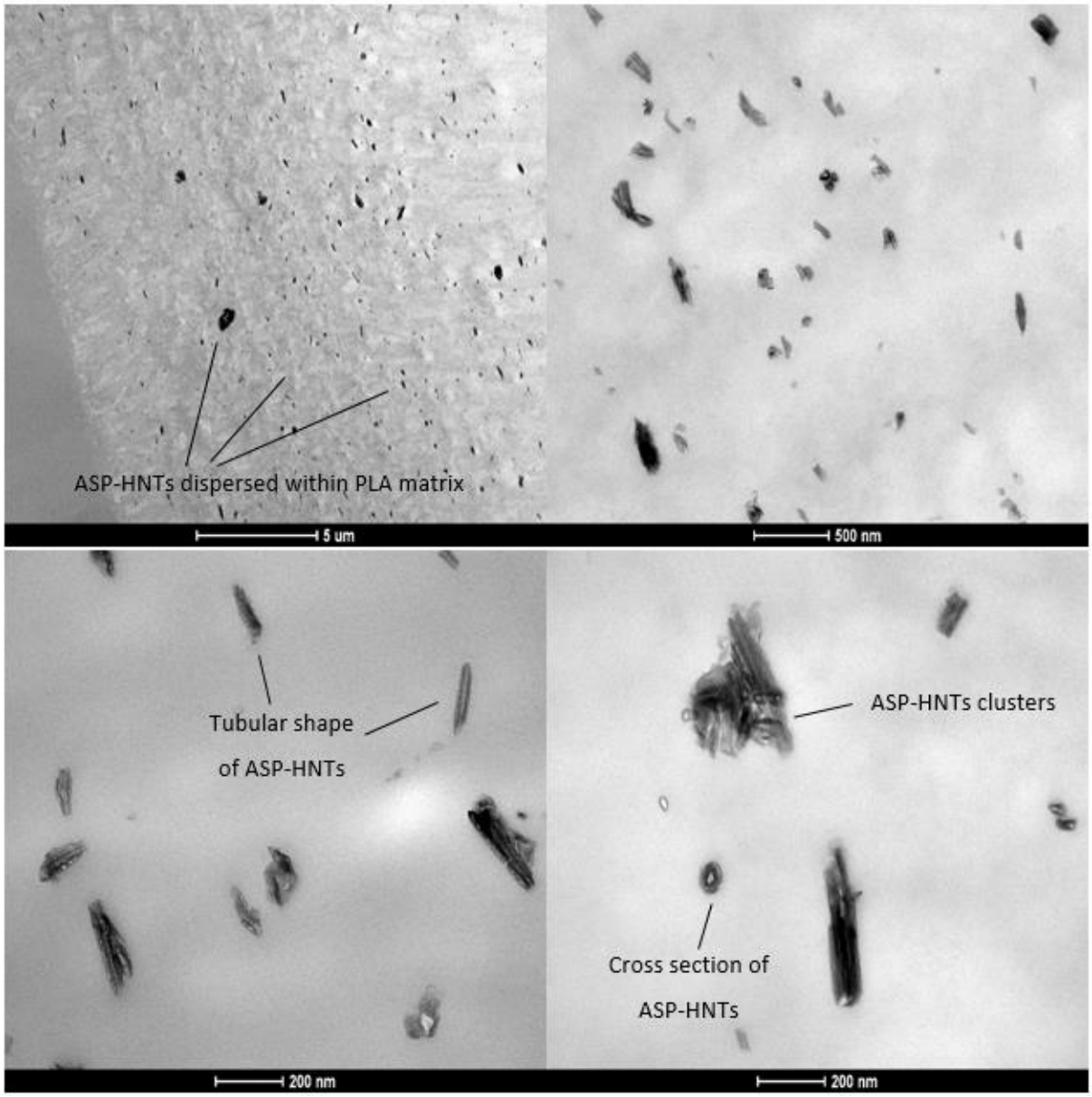

Figure 3: TEM images of ASP modified HNTs dispersed well within PLA matrix. The tubular shape of ASP- HNTs and some small clusters can be clearly seen

3.5 surface wettability

Contact angle measurements indicated that the incorporation of 1 - 5wt% ASP-HNTs did not have a significant effect on the surface wettability of PLA ($p = 0.396$) and the contact angle remained at $74.9 \pm 8°$.

3.6 Thermogravimetric analysis

Thermal degradation of PLA/ASP-HNTs composites was investigated by TGA and shown in figure 4. PLA degraded without forming any residue, while PLA/ASP-HNTs composites left residue of ASP-HNTs. Compared to virgin PLA, the addition of ASP-HNTs to PLA matrix reduced the thermal stability of the PLA. The temperarature at 5% and 10% weight loss and the onset temperature were reduced dramatically from 379.6 °C, 391.1 °C and 397.7 °C of virgin PLA to 299.4 °C, 307.8 °C and 311.4 °C of PLA/ASP-HNTs 1wt% respectively. In addition, the thermal stability did not deteriorate any further with increasing content of ASP-HNTs.

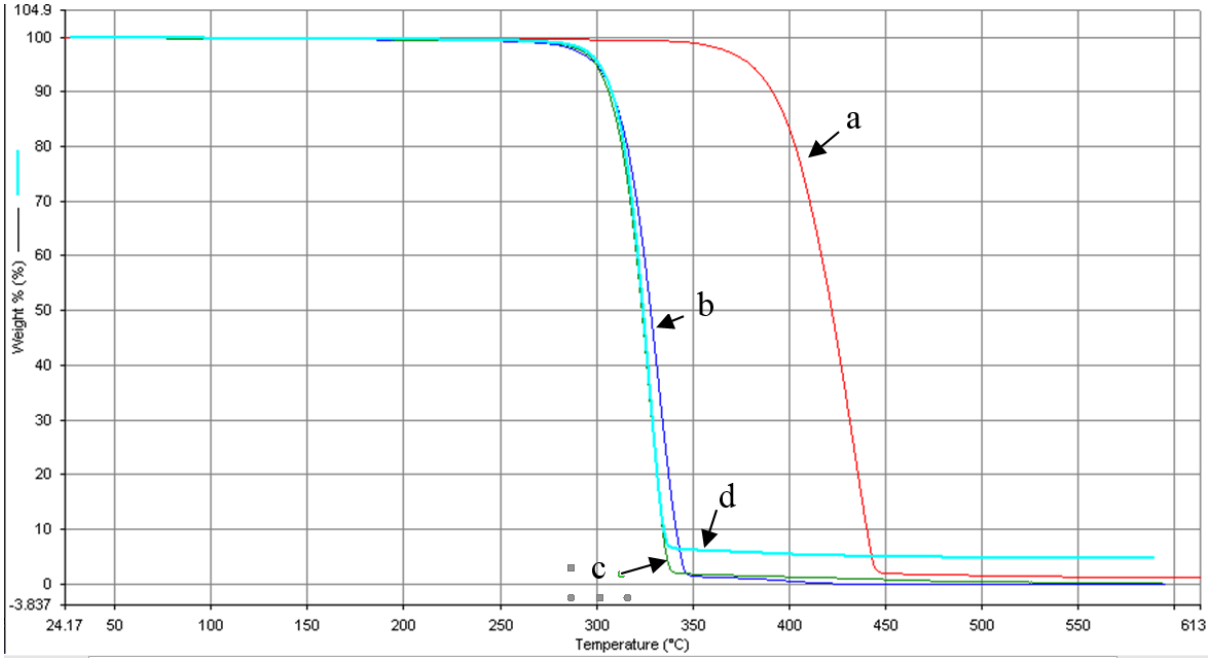

Figure 4: TGA curves of PLA/ASP-HNTs composites, a: virgin PLA, b: PLA/ASP-HNTs 1wt%, c: PLA/ASP-HNTs 2wt%, d: PLA/ASP-HNTs 5wt%.

3.7 Mechanical testing

The tensile testing results showed that there was no significant difference in Young's modulus between PLA and PLA/ASP-HNTs 1wt% ($p = 0.13$), but an increase was shown in composites with 2wt% and 5wt% of both HNTs and ASP-HNTs ($p < 0.05$ for all comparison). However, the percentage of strain at max load was not affected ($p = 0.903$ for all comparison). It was found out that ASP-HNTs displayed a better reinforcing effect than unmodified HNTs, shown in figure 5. Young's modulus of PLA/ASP-HNTs 2wt% was higher than that of PLA/HNTs 2wt% ($p < 0.05$). Similarly, Young's modulus of PLA/ASP-HNTs 5wt% was higher than that of PLA/unmodified HNTs 5wt% blend ($p < 0.019$).

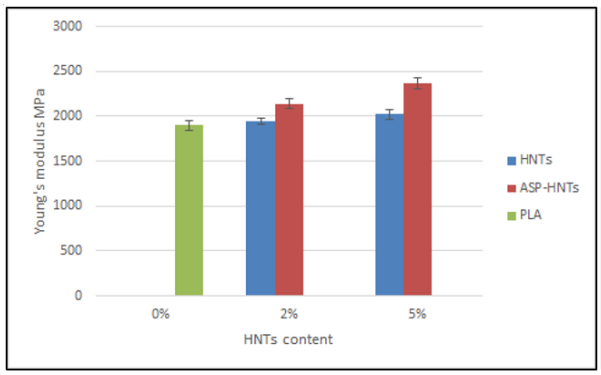

Samples	Young's Modulus (MPa)	Percentage Strain at Maximum Load
PLA	1898 ± 56.95	3.1 ± 0.86
PLA/HNT2%	1947 ± 101	4.1 ± 0.81
PLA/ASP-HNT2%	2143 ± 175.71	3 ± 0.54
PLA/HNT5%	2026 ± 174.99	2.6 ± 0.74
PLA/ASP-HNT5%	2369 ± 174.47	2.9 ± 0.56

Figure 5: Young's modulus of PLA and PLA composites ($p<0.05$ for all comparison)

3.8 Hemolysis

The hemolysis rates (HR) of PLA and PLA composites samples are shown in figure 6. The hemolysis rates range from 0.1 to 1.3%. According to ASTM-F756, it is blood compatible when hemolysis rate is lower than the 5% threshold [23]. Therefore, all the samples have an excellent blood compatibility. There was no significant difference between them ($p > 0.05$ for all comparison).

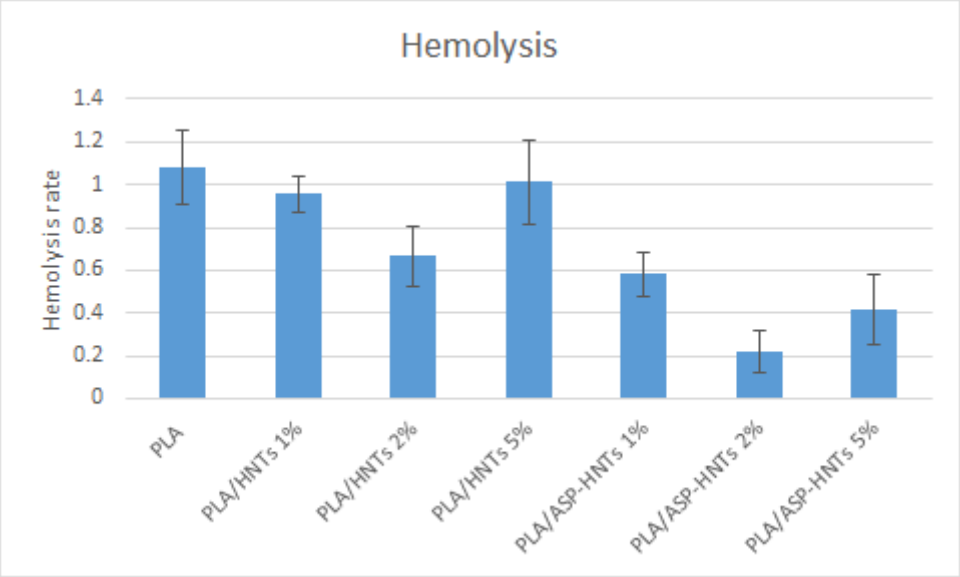

Figure 6: Hemolysis rate of PLA and PLA composites.

3.9 Extract contact cell viability test-MTT assay

Figure 7 illustrated the viability of HUVECs cultured for day 2 and 6 after been treated with extract of PLA and PLA composites. The ISO 10993 standard stated that reduction of cell viability by more than 30% is considered a cytotoxic effect [21]. The tested cell viability of PLA and PLA composites indicated that all the test samples were cytocompatible and there was no significant difference between the test samples ($p > 0.05$ for all comparison). Cells all looked healthy, and there was no obvious morphological changes for all the cells that have been treated with extract of PLA and PLA composites. Cellular debris can be spotted due to natural waste production and HUVECs can produce moderate or heavy debris stated by the supplier.

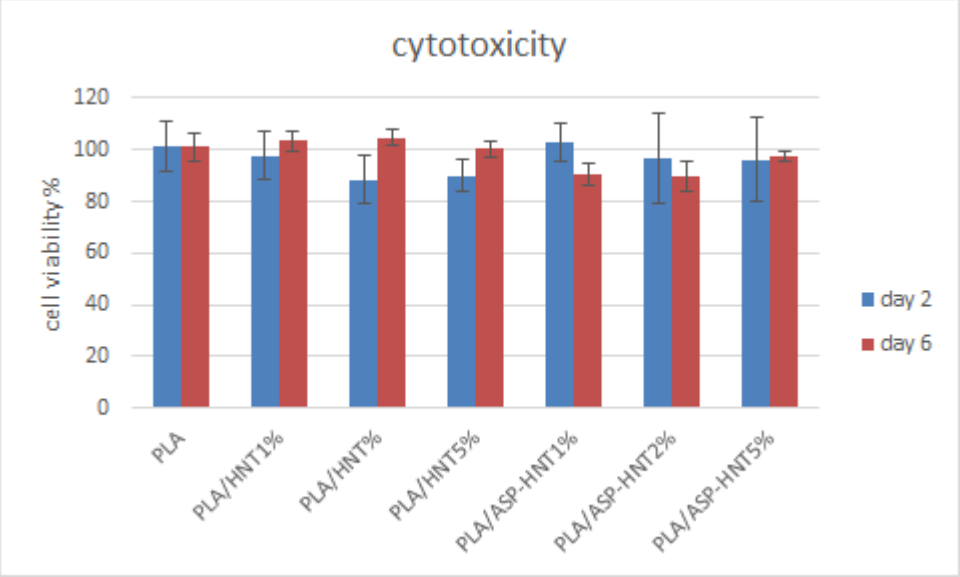

Figure 7: Cell viability of PLA and PLA composites after 2 and 6 days incubation.

3.10 In vitro degradation testing

Hydrodegradation of PLA results in molecular weight reduction, changes in chemical structures and thus impaired mechanical properties. Hence the degradation behaviour of PLA/ASP-HNTs 2wt% composites was investigated by GPC, FTIR, weight loss measurement, tensile testing and DSC. GPC results showed that number average molecular weight (Mn) and

weight average molecular weight (Mw) reduced throughout the degradation period from 3.3×10^6 (Mn) and 4.3×10^6 (Mw) at the beginning of the degradation process to 2.59×10^6 and 3×10^6 with 23.6% and 30.6% reduction respectively by the end of the degradation process. The broadness of molecular weight distribution remained unchanged with polydispersity index of 1.18 ± 0.1 (Table 2).

Table 2: GPC results for PLA/ASP-HNTs composites during the degradation process

Week	Mw	Mn	D = Mw/Mn
0	4323064	3389422	1.275457585
1	3709657	3283921	1.129642583
2	4507167	3753817	1.200689059
4	3700608	3092199	1.196756095
9	3450960	3039164	1.135496472
12	3442786	3060319	1.124976187
16	3426369	2854227	1.200454274
20	3315665	2847232	1.164522245
24	3000670	2590116	1.158507959

Chemical structure changes during degradation process were investigated by FTIR spectroscopy. Several new peaks started appearing from the 12th week of degradation, including O-H stretching at 3185 cm^{-1} and N-H deformation at 1552 cm^{-1} and 1630 cm^{-1} [16]. The carbonyl group C=O band at 1750 cm^{-1} and C-O band between 1000-1300 cm^{-1} related to ester bond did not change throughout the degradation process.

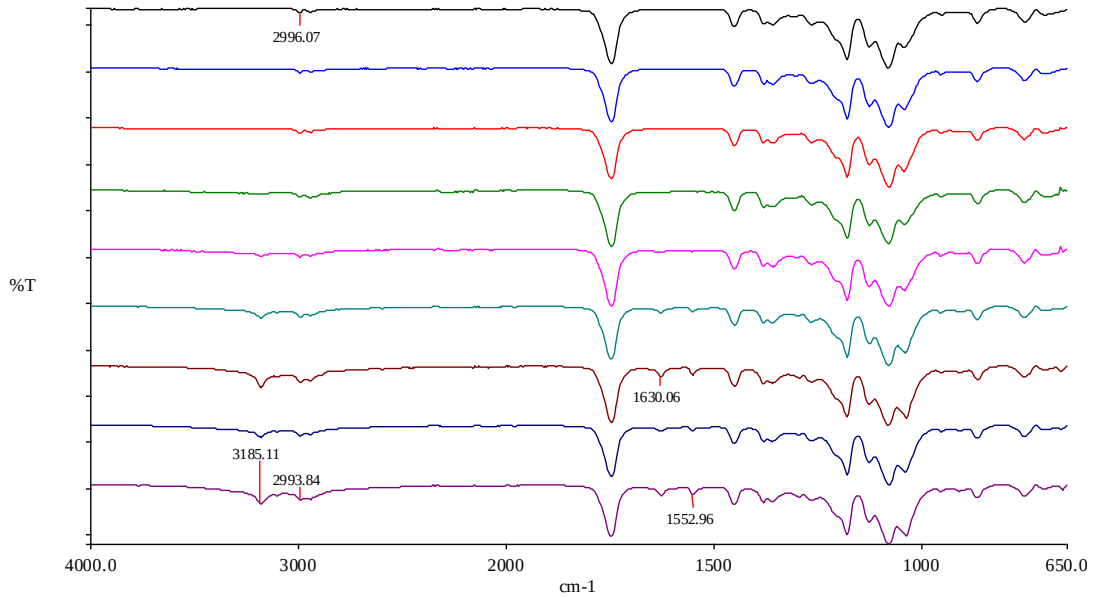

Figure 8: FTIR curves of PLA/ASP-HNTs composites during degradation process (From top to bottom: 0, 1, 2, 4, 9, 12, 16, 20 and 24 weeks).

The mass reduction of PLA/ASP-HNTs composites was studied along with PLA and PLA/HNTs composites. None of the samples displayed a weight loss in the first 12 weeks in SBF, PLA/ASP-HNTs composites showed the highest weight loss of 5.7, 8.2 and 12.1% by the end of 12th, 20th and 24th week of degradation, compared to PLA with 1.9, 1.2 and 2.6%, and PLA/HNTs with 1.6, 2 and 3.1% respectively (Figure 9). However, with the highest weight loss, PLA/ASP-HNTs samples remained the strongest by the end of the 24th week (Figure 9). Young's modulus of PLA/ASP-HNTs composites displayed a consistent reduction during the degradation process with 1583.4 ± 190 MPa and 26% loss by the end of the 24th week of degradation, while PLA samples showed a sudden reduction in Young's modulus in the 24th

week of degradation period with 1259.1 ± 184MPa and 33.7% loss, and PLA/HNTs samples retained a Young's modulus of 1409.4 ± 81.8MPa and 27.6% loss by the end of the 24th week of degradation.

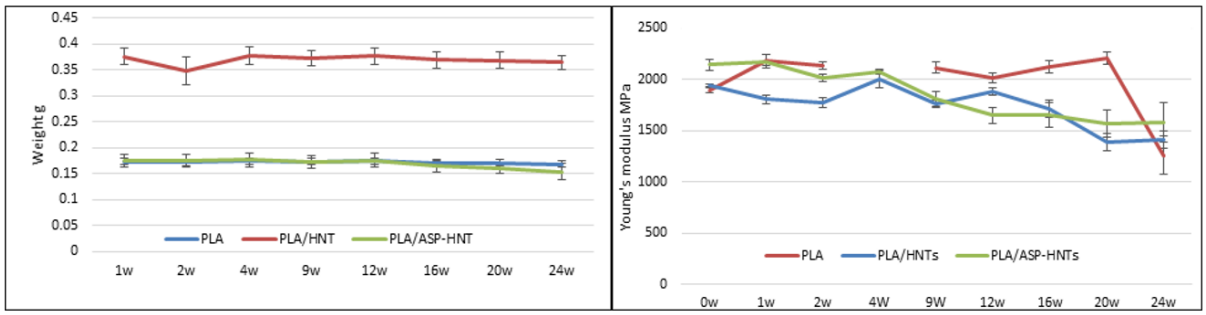

Figure 9: Weight measurement and tensile testing results of PLA and PLA composites during degradation process.

The thermal analysis from DSC test revealed that the T_g of PLA/ASP-HNTs nanocomposite remained unchanged during the degradation process. Cold crystallization temperature (T_{cc}) shifted lower slightly from 113°C at the 1st week to 110°C by the 24th week of degradation. Two melting peaks (T_m) appeared at the 1st week of the degradation and the second peak slowly reverted to a shoulder on the main T_m peak in the 12th, 16th, 20th and 24th week of degradation, and the main melting peak remained unchanged (Figure 10).

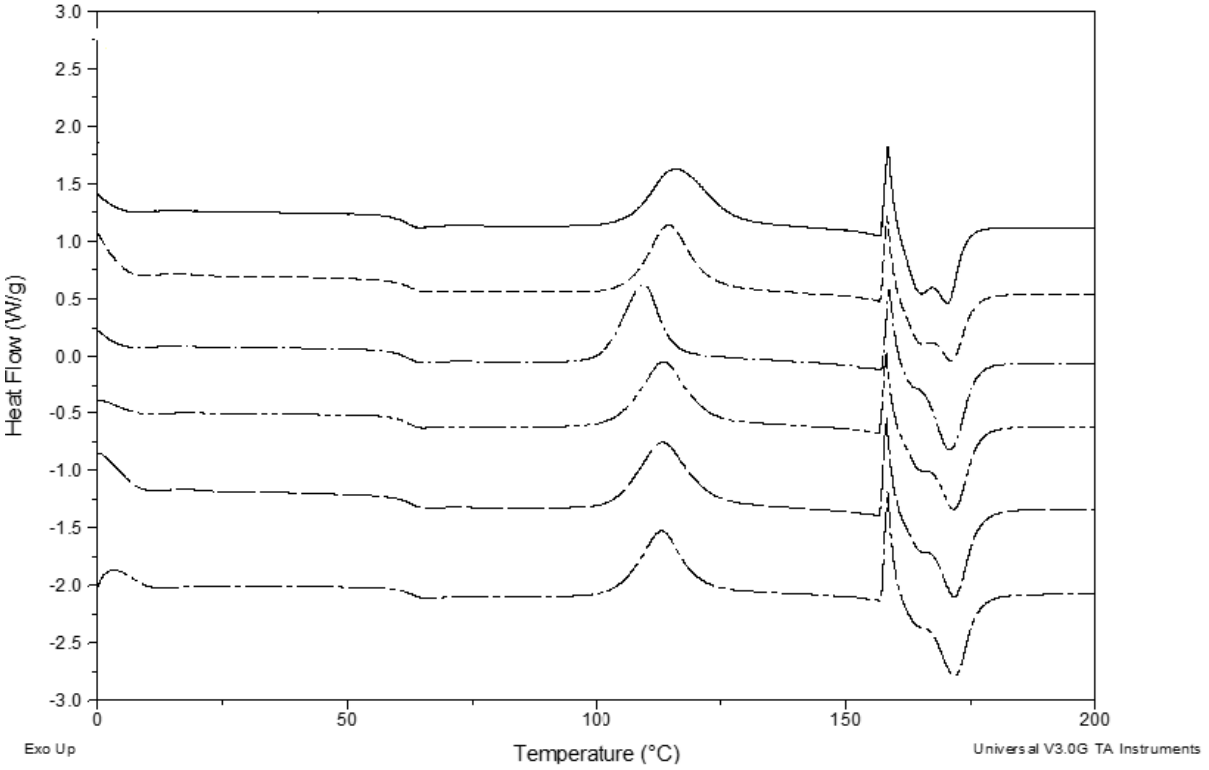

Figure 10: DSC curves of PLA/ASP-HNTs composites during degradation process (From top to bottom: 1, 2, 12, 16, 20 and 24 weeks).

4. Discussion

Surface modified HNTs were melt compounded with PLA matrix in this study to improve the adhesion between HNTs and PLA matrix in order to optimize the reinforcing effect of HNTs, since the adhesion between filler and polymer matrix plays a fundamental role in reinforced composites [29]. DSC results indicated that ASP-HNTs acted as nucleating agents in PLA/ASP-HNTs composites, evidenced by the consistent increase of the degree of crystallinity

with increasing content of ASP-HNTs in PLA/ASP-HNTs composites. The PLA/ASP-HNTs composites could crystallize quicker than virgin PLA. However, the T_{cc} of PLA/ASP-HNTs composites reduced compared to virgin PLA, indicating that heterogeneous nucleation was likely to occur, where thinner or less perfect crystalline lamella was formed compared to that of virgin PLA. The nucleating effect and heterogeneous nucleation have also been reported by Haroosh et al. in their study of PLA/PCL blends with ASP modified HNTs [16].

The appearance of new peaks of N-H deformation and C-H stretching in FTIR spectra due to added ASP confirmed the chemical interaction between ASP and HNTs. Similar new peaks and corresponding bondings were reported by Yuan et al. in the study of ASP treated kaolinite samples [30]. Pasbakhsh et al. modified HNTs with glycidyl methacrylate (GMA), which shared a similar modificiation mechanism as ASP, grafting GMA on Al-OH groups of HNTs, introducing new O-H bond and producing Al-O-CH_2 group. Therefore, similar FTIR new peaks of C-H bend and O-H stretching reported by Pasbakhsh were also found in this current study [31].

TEM images of PLA/ASP-HNTs composites indicated that ASP modified HNTs dispersed better within PLA matrix, compared with our previous study in unmodified HNTs within PLA [12]. This is because that ASP was grafted on the surface of HNTs and reduced the content of hydroxyl group on the surface of HNTs, thus reduced hydrophobicity of HNTs, which helped HNTs to disperse in polymer matrix [14]. The degree or uniformity of dispersion of filler within polymer matrix determines the final mechanical properties of the composite. Aggregated fillers usually act as stress concentration point where fracture usually happens, deteriorating the mechanical properties. However, compared to our previous study, where large aggregates of unmodified HNTs and voids can be clearly seen in the SEM image at 500 magnification, the dispersion and contact between ASP modified HNTs and PLA in this current study appeared to be greatly improved. A combination of well dispersed ASP-HNTs in PLA matrix and small amount of HNTs clusters were visible in TEM images. Similar finding was reported by Prashantha *et al*. who investigated unmodified HNTs and quaternary ammonium salt treated (QM-HNTs) compounded with polypropylene, and found that a better dispersion in the case of QM-HNTs compared to unmodified HNTs [15]. It is important to note that surface modification is not the only method to improve HNTs dispersion within polymer matrix. A low screw speed of 35 rpm was adopted in this study due to PLA stiffness and desk top extruder. It is possible that with higher screw speed and resulted higher shear force, the dispersion of HNTs with polymer matrix can be improved.

PLA/ASP-HNTs composites were tested to be hydrophobic in this study with no change in contact angle between distilled water and composite surface with increasing content of modified HNTs, which was consistent with our previous study of PLA/unmodified HNTs composites [12]. Cavallaro et al. found that well dispersed HNTs in hydrophobic low methoxyl pectin can result in a hydrophilic composite, and the incorporation of HNTs into hydroxypropylcellulose matrix improved wettability of hydroxypropylcellulose/HNTs composite [32]. They also found out that the introduction of HNTs to pectin and hydrophilic polyethylene glycol (PEG) blend formed a hydrophobic composite due to the increase of the surface roughness. Most importantly, they found that HNTs loading can affect the surface roughness of the composite, and with 10wt% HNTs loading, the surface of composite was rough and reckoned as hydrophobic, while 30wt% HNTs loading decreased the surface roughness, thus reduced the hydrophobicity [33]. Very small amounts of HNTs were used in this study, and the hydrophobicity of PLA was not affected by the addition of HNTs.

In comparison to virgin PLA, the decreased onset temperature of PLA/ASP-HNTs composites from TGA results indicated that the introduction of ASP-HNTs to PLA matrix reduced the

thermal stability of PLA. This finding was consistent with previous study of PLA and unmodified HNTs nanocomposites [12]. The influence of clay in thermal stability of polymer has been studied extensively. Generally, the thermal stability of polymer matrix can be improved by a high concentration of clay content (10 wt%), whereas no effect on thermal stability of the polymer matrix was found with lower clay content (up to 5 wt%) [34]. Liu et al. reported improved thermal stability in PLA/HNTs composites with up to 40 wt% HNTs loading [27], and the mechanism was explained that HNTs acted as heat resistant barrier since HNTs have higher thermal degradation stability than PLA, and the degradation product of PLA can enter the lumens of HNTs [14]. Similarly, Ismail et al. reported a significant improvement in thermal stability in HNTs filled ethylene propylene diene monomer nanocomposites, but the temperature at 5% weight loss didn't increase until the HNTs loading was increased up to 15% [35]. However, a negative effect of thermal stability of PLA composites was found in this and previous studies. Similiarly, Russo et al. also reported that the addition of HNTs with 1, 3 and 5 wt% loading led to a decrease in thermal stability of PLA and this effect was enhanced with the clay content [36]. The results might be related to the formation of water during PLA/ASP-HNTs compounding, which led hydrolysis. Kopinke et al. have explained the occurrence of oxygen-centred or carbon-centred radicals due to cleavage of alkyl-oxygen or acyl-oxygen bonding in ester during hydrolysis [37].

PLA is a relatively strong biodegradable polymer with reported tensile strength of 50-70 MPa, Young's modulus of 3-4 GPa and elongation at break of 2-10% [38]. In this study observed results were 52.33 ± 16.89 MPa for stress at maximum load, 1.898 ± 56.95 GPa for Young's modulus and 3.1 ± 0.86 % for percentage strain at maximum load by tensile testing. The introduction of HNTs significantly increased Young's modulus of PLA in previous work [12]. This is because high aspect ratio of HNTs helps reinforce polymers in composites by optimizing the load transfer from the matrix to the nanotubes, and the elastic modulus of HNTs is 140GPa [14]. It was found that ASP-HNTs have a better reinforcing effect than unmodified HNTs in the current study. Unmodified HNTs increased Young's modulus of PLA by 2.6% and 6.7% with 2wt% and 5wt% HNTs loading respectively, while ASP-HNTs increased by 12.9% and 25% with 2wt% and 5wt% ASP-HNTs loading respectively. Similar better reinforcing effects of modified HNTs were also reported with various polymers [15–17]. The better reinforcing effect of ASP modified HNTs than unmodified HNTs can be explained by better dispersion of ASP-HNTs with in PLA matrix than unmodified HNTs, causing increased contact surface between ASP-HNTs and PLA matrix.

According to ISO 10993 standard, all blood contacting medical devices are required to have hemolysis tests completed. Hemolysis rates of all PLA and PLA composites in this study were well below 5% threshold, therefore, all samples were considered non-hemolytic. The addition of HNTs and ASP modified HNTs did not change the hemocompatibility of PLA. These results were in close agreement with that obtained by Liu et al. who investigated hemocompatibility of HNTs [39]. It is worthwhile to point out that PLA has long safety history in blood contacting applications, for instance, poly DL-lactic acid (PDLLA) has been used as drug carrier coated on the surface of the drug eluted stents, with the degradation of PDLLA the drug sirolimus can be released during a period of 3 to 4 months [40].

The PLA and PLA composites were found to be non-toxic to HUVEC cells according to the MTT test results. High molecular weight PLA, that has been used in medical applications, has reported with a very good biocompatibility [41]. HNTs have been reported as a drug delivery vehicle [42] and the biocompatibility of HNTs has been extensively investigated. Liu et al. reported that HNTs exhibit good cell compatibility in low concentration range, but high concentration of HNTs may cause DNA breakage and result latent toxicity effects [39]. The HNTs used in this study was at very low concentration.

Hydrolytic degradation of PLA/ASP-HNTs composites was investigated in this study. As an aliphatic polyester, the cleavage of the ester linkages in PLA by absorbed water produces a successive reduction in molecular weight, in figure 11.

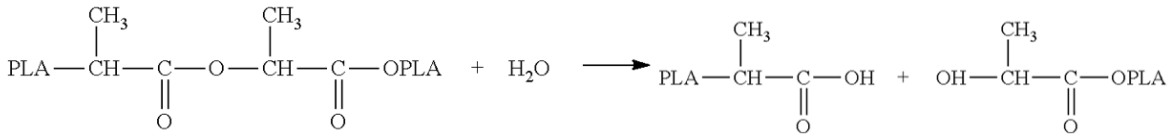

Figure 11: Hydrolytic degradation of PLA

The GPC results revealed that the molecular weight of PLA/ASP-HNTs composites was reduced by 23.6% (Mn) and 30.6% (Mw) at the end of the 24th week of degradation. Valapa et al. also reported a similar reduction in molecular weight during degradation process, and they concluded that the nanofillers and elevated temperature can lead to high molecular weight reduction, due to enhanced chain mobility of PLA molecular chains [43]. However, the molecular weight distribution was not significantly changed through the degradation process, which indicated that bulk degradation had not begun in this study.

FTIR spectra of PLA/ASP-HNTs composites during degradation process also confirmed that bulk degradation didn't occur. From the 9th week of degradation process new peaks of N-H deformation related to ASP-HNTs started appearing, indicating the ASP-HNTs filler leached out from PLA matrix and surface erosion happened. However, the ester bond of PLA did not change during the degradation process, evidenced by the unchanged carbonyl group C=O band at 1750 cm^{-1} and C-O band at 1000-1300 cm^{-}1. As ester group cleavage is the primary degradation mechanism of PLA, it can be concluded that the major degradation process had not begun at the 24th week of degradation.

During degradation process the mass of PLA, PLA/HNTs and PLA/ASP-HNTs composites only reduced slightly as expected due to the hydrophobic nature of PLA and PLA composites. PLA/ASP-HNTs composites displayed the highest reduction in weight loss with 12.1% by the end of the 24th week of degradation, followed by PLA/HNTs composites with 3.1% and PLA with 2.6%. This increased degradation rate could be related to the heterogeneous nature of the composite structure which allowed easier water permeation. Similar weight loss has been reported with 2% in PLA and 8.6% in PLA/TiO composites by 70 weeks of degradation process [44]. Li et al. also claimed that the degradation rate of most PLA composites was faster than that of the neat PLA [45].

PLA/ASP-HNTs composites retained 74% of its Young's modulus by the 24th week of degradation, while PLA/HNTs composites and PLA kept 72.4% and 66.3% respectively. This may be explained by the fact that during polymer degradation, the amorphous regions degrade first and the mechanical properties of the polymer were retained by the crystalline regions. The molecules in the amorphous region are loosely packed, and thus make it more susceptible to degradation, while the crystalline part of the polymers is more resistant to degradation than the amorphous region [46]. PLA/ASP-HNTs composites displayed a consistent and gradual reduction in Young's modulus, which complied with the gradual reduction in molecular weight from GPC results, and this finding was also reported by Vieira et al. in PLA-PCL fibre *in vitro* degradation study [47]. PLA/ASP-HNTs composites remained the strongest while degraded the fastest among PLA and PLA/HNTs composites, which is beneficial for fully biodegradable coronary stents, as the stents are required to keep the vessel open while the vessel is healing and remodelling for the first 6 months, and not to interfere with luminal enlargement of blood vessels, which often takes place between 6 months and 5 years after angioplasty [7]. PLA has a c.a. 2 years degradation period [48], but it has been reported that implants made from PLA didn't disappear in this time frame and caused foreign body reaction [49]. Therefore, the

PLA/ASP-HNTs composites with high degradation rate while retaining mechanical strength may prove beneficial for use in biodegradable coronary stents.

It is claimed that the degradation process can be classified into two stages: random hydrolytic scission of ester bonds in the amorphous region, where the T_m remained constant, and hydrolytic attack of the crystalline domain with drop in T_m [50]. The unchanged T_m of PLA/ASP-HNTs composites in this study indicated that the crystalline region of PLA composites hasn't hydrolytically degraded yet. Two T_m on DSC curves are ascribed to the melting of crystalline regions of various size formed during cooling and crystallisation process. The lower T_m is associated to the melting of the smaller crystals produced by secondary crystallization, whereas the higher T_m corresponds to the melting of the major crystals formed in the primary crystallization process [51]. The reduction in T_m observed in the 12^{th}, 16^{th}, 20^{th} and 24^{th} week of degradation might indicate the degradation of the smaller crystals in the composites. Similar change in bimodal melting peaks was reported by Luo et al. [44]. The lower T_{cc} of PLA/ASP-HNTs composites could be related to the reduction in molecular weight during the degradation process, because shorter chains would tend to crystallize at lower temperature, which has also reported by Valapa et al. [43].

5. Conclusion

ASP-HNTs was melt compounded in a PLA matrix in this study. ASP-HNTs dispersed better within the matrix as observed by TEM, thus displayed better reinforcing effect in PLA composites, compared to unmodified HNTs. The Young's modulus of PLA was increased by 25% with 5wt% ASP-HNTs loading, while this value was 12.9% with 5wt% for untreated HNTs. DSC thermographs indicated that ASP-HNTs acted as nucleating agents and increased crystallisation of PLA/ASP-HNTs composites. All PLA and PLA nanocomposites were found to be blood and cell compatible. *In vitro* degradation studies revealed that ASP-HNTs appeared to increase the degradation process of PLA compared to PLA and PLA/HNTs samples. However, PLA/ASP-HNTs composites retained the highest Young's modulus by the 24^{th} week of degradation, which was the result of well dispersion of ASP-HNTs in PLA matrix. The consistent and gradual reduction in mechanical strength of PLA/ASP-HNTs composites was in connection with its molecular weight reduction. However, the degradation in crystalline region of PLA/ASP-HNTs composites didn't occur, evidenced by the unchanged T_m of PLA/ASP-HNTs composites from DSC thermograms, which also explained the reason why PLA/ASP-HNTs retained 74% of Young's modulus by the end of the degradation period. In addition, the unchanged ester group peaks in FTIR spectra revealed the primary degradation process of PLA/ASP-HNTs composites had not yet occur. A period of 6 months is critical for blood vessel remodelling, so the experiment was designed to have a degradation of 6 months. But it is worthwhile to investigate a longer period to observe the bulk degradation in the future research, as well as perspective of size and bioresorption, to shorten the experimental period, the accelerated degradation can be achieved with elevated temperatures [52]. The results from the current study indicated that the reinforced PLA/ASP-HNTs composites could be potentially used in long term biological applications that require high strength for up to 6 months but thereafter degrade, such as coronary stent.

Acknowledgement

This work has been funded by the President's Seed Fund from Athlone Institute of Technology. Halloysite nanotubes were kindly donated by Applied Minerals Inc.

Disclosures

The authors declare that there is no conflict of interests regarding the publication of this article, this manuscript has not been published elsewhere and it has not been submitted simultaneously for publication elsewhere.

References

[1] Y. Chen, Marcelo Jorge Carvalcanti De Sa, M. Dalton, D.M. Devine, Biodegradable medical implants, in: D.M. Devine (Ed.), Bioresorbable Polym. Their Biomed. Appl., Smithersrapra, 2017: pp. 27–76. https://www.smithersrapra.com/publications/books/latest-releases/bioresorbable-polymers-and-biomedical-applications (accessed October 18, 2017).

[2] C.K.S. Pillai, C.P. Sharma, Review paper: absorbable polymeric surgical sutures: chemistry, production, properties, biodegradability, and performance., J. Biomater. Appl. 25 (2010) 291–366. doi:10.1177/0885328210384890.

[3] M. Suchenski, M.B. McCarthy, D. Chowaniec, D. Hansen, W. McKinnon, J. Apostolakos, R. Arciero, A.D. Mazzocca, Material Properties and Composition of Soft-Tissue Fixation, Arthrosc. - J. Arthrosc. Relat. Surg. 26 (2010) 821–831. doi:10.1016/j.arthro.2009.12.026.

[4] M.S. Nuzzo, M. Posner, W.J. Warne, F. Medina, R. Wicker, B.D. Owens, Compression force and pillout strength comparisonk of bioabsorbable implants for osteochondral lesion fixation, Am. J. Orthop. April (2011) 61–63.

[5] E. Lih, S.H. Oh, Y.K. Joung, J.H. Lee, D.K. Han, Polymers for cell/tissue anti-adhesion, Prog. Polym. Sci. 44 (2015) 28–61. doi:10.1016/j.progpolymsci.2014.10.004.

[6] Y. Onuma, P.W. Serruys, Role of imaging in the implantation of bioresorbable scaffolds in coronary stenoses, in: J. Escaned, P.W. Serruys (Eds.), Coron. Stenosis Imaging, Struct. Physiol., 2nd editio, Europa Digital Publishing, 2015. http://www.pcronline.com/eurointervention/textbook/coronarystenosis/chapter/?chapter_id=184 (accessed January 20, 2016).

[7] J.A. Ormiston, P.W.S. Serruys, Bioabsorbable coronary stents, Circ. Cardiovasc. Interv. 2 (2009) 255–260. doi:10.1161/CIRCINTERVENTIONS.109.859173.

[8] M. O'Riordan, The Bioresorbable Stent Story So Far: What Promise? What Price?, TCTMD. (2016) August 17. http://www.tctmd.com/show.aspx?id=136055&utm_source=Spotlight&utm_medium=email&utm_campaign=Spotlight_081816 (accessed August 19, 2016).

[9] C. Agrawal, K. Haas, D. Leopold, H. Clark, Evaluation of poly(L-lactic acid) as a material for intravascular polymeric stents, Biomaterials. 13 (1992) 176–182. doi:10.1016/0142-9612(92)90068-Y.

[10] Boston scientific, Synergy everolimus-eluting platinum chromium coronary stent system General Specifications and Materials List, Bost. Sci. (2015).

[11] V. Farooq, B.D. Gogas, P.W. Serruys, Restenosis: Delineating the numerous causes of drug-eluting stent restenosis, Circ. Cardiovasc. Interv. 4 (2011) 195–205. doi:10.1161/CIRCINTERVENTIONS.110.959882.

[12] Y. Chen, L.M. Geever, J.A. Killion, J.G. Lyons, C.L. Higginbotham, D.M. Devine, Halloysite nanotube reinforced polylactic acid composite, Polym. Compos. (2015) DOI 10.1002/pc.23794. doi:10.1002/pc.23794.

[13] P. Yuan, D. Tan, F. Annabi-Bergaya, Properties and applications of halloysite

nanotubes: recent research advances and future prospects, Appl. Clay Sci. 112–113 (2015) 75–93. doi:10.1016/j.clay.2015.05.001.

[14] M. Liu, Z. Jia, D. Jia, C. Zhou, Recent advance in research on halloysite nanotubes-polymer nanocomposite, Prog. Polym. Sci. 39 (2014) 1498–1525. doi:10.1016/j.progpolymsci.2014.04.004.

[15] K. Prashantha, M.F. Lacrampe, P. Krawczak, Processing and characterization of halloysite nanotubes filled polypropylene nanocomposites based on a masterbatch route: effect of halloysites treatment on structural and mechanical properties, Express Polym. Lett. 5 (2011) 295–307. http://www.expresspolymlett.com/articles/EPL-0001728_article.pdf (accessed July 21, 2015).

[16] H.J. Haroosh, Y. Dong, D.S. Chaudhary, G.D. Ingram, S.I. Yusa, Electrospun PLA: PCL composites embedded with unmodified and 3-aminopropyltriethoxysilane (ASP) modified halloysite nanotubes (HNT), Appl. Phys. A Mater. Sci. Process. (2013). doi:10.1007/s00339-012-7233-7.

[17] S. Deng, J. Zhang, L. Ye, Effects of chemical treatment and mixing methods on fracture behaviour of halloysite-epoxy nanocomposites, Proc. 17th Int. Conf. 'Composite Mater. (2009). http://iccm-central.org/Proceedings/ICCM17proceedings/Themes/Nanocomposites/NANOCLAY-NANOSILICATE COMP/E4.1 Deng.pdf.

[18] Shin-Etsu Chemical Ltd., Silane Coupling Agents, Silane Coupling Agents. (2015) 1–24. http://www.shinetsusilicone-global.com/catalog/pdf/SilaneCouplingAgents_e.pdf (accessed December 4, 2015).

[19] D.R. Silva, P. Pasbakhsh, K. Goh, S.-P. Chai, J. Chen, Synthesis and characterisation of poly (lactic acid)/halloysite bionanocomposite films, J. Compos. Mater. 48 (2013) 3705–3717. doi:10.1177/0021998313513046.

[20] H. Masuda, S. Ishihara, I. Harada, T. Mizutani, M. Ishikawa, K. Kawabata, H. Haga, Coating extracellular matrix proteins on a (3-aminopropyl)triethoxysilane-treated glass substrate for improved cell culture, Biotechniques. 56 (2014) 172–179. http://www.biotechniques.com/BiotechniquesJournal/2014/April/Coating-extracellular-matrix-proteins-on-a-3-aminopropyltriethoxysilane-treated-glass-substrate-for-improved-cell-culture/biotechniques-351247.html (accessed December 4, 2015).

[21] ISO-10993-5, ISO.10993. PART 5. Biological evaluation of medical devices. Tests for in vitro cytotoxicity, ISO. (2009).

[22] ISO-10993-12, International organization for standardization, ISO.10993. Part 12 Sample preparation and reference materials, ISO. (2012).

[23] ASTM F 756 - 00, Standard Practice for Assessment of Hemolytic Properties of Materials, (2000). www.astm.org.

[24] S. Jana, S. Das, C. Ghosh, A. Maity, M. Pradhan, Halloysite Nanotubes Capturing Isotope Selective Atmospheric CO2, Sci. Rep. 5 (2015) 8711. doi:10.1038/srep08711.

[25] S. Kumar-Krishnan, A. Hernandez-Rangel, U. Pal, O. Ceballos-Sanchez, F.J. Flores-Ruiz, E. Prokhorov, O. Arias de Fuentes, R. Esparza, M. Meyyappan, Surface functionalized halloysite nanotubes decorated with silver nanoparticles for enzyme immobilization and biosensing, J. Mater. Chem. B. 4 (2016) 2553–2560. doi:10.1039/C6TB00051G.

[26] S. Suzuki, Y. Ikada, S. Detyothin, A. Kathuria, W. Jaruwattanayon, S.E.M. Selke, R. Auras, Poly(Lactic Acid), in: R. Auras, L.-T. Lim, S.E.M. Selke, H. Tsuji (Eds.), POLYLACTIC ACID Synth. Struct. Prop. Process. Appl., John Wiley & Sons, Inc., Hoboken, NJ, USA, 2010: pp. 227–271.

[27] M. Liu, Y. Zhang, C. Zhou, Nanocomposites of halloysite and polylactide, Appl. Clay Sci. 75–76 (2013) 52–59. doi:10.1016/j.clay.2013.02.019.

[28] Y. Chen, L.M. Geever, J.A. Killion, J.G. Lyons, C.L. Higginbotham, D.M. Devine, Review of Multifarious Applications of Poly (Lactic Acid), Polym. Plast. Technol. Eng. 55 (2016) 1057–1075. doi:10.1080/03602559.2015.1132465.

[29] K. Prashantha, M.-F. Lacrampe, P. Krawczak, Halloysite Nanotubes-Polymer Nano composites:A New Class of Multifaceted Materials, Adv. Mater. Manuf. Charact. Vol3 Issue. 1 (2013) 11–14. doi:10.11127/ijammc.2013.02.003.

[30] P. Yuan, P.D. Southon, Z. Liu, M.E.R. Green, J.M. Hook, S.J. Antill, C.J. Kepert, Functionalization of halloysite clay nanotubes by grafting with aminopropyltriethoxysilane, J. Phys. Chem. C. 112 (2008) 15742–15751. doi:10.1021/jp805657t.

[31] P. Pasbakhsh, H.K. How, C.S. Piao, Modification of halloysite nanotubes with glycidyl methacrylate, in: Aust. Regolith Clays Conf. Midura, 2012.

[32] G. Cavallaro, D.I. Donato, G. Lazzara, S. Milioto, Films of Halloysite Nanotubes Sandwiched between Two Layers of Biopolymer: From the Morphology to the Dielectric, Thermal, Transparency, and Wettability Properties, J. Phys. Chem. C. 115 (2011) 20491–20498. doi:10.1021/jp207261r.

[33] G. Cavallaro, G. Lazzara, S. Milioto, Sustainable nanocomposites based on halloysite nanotubes and pectin/polyethylene glycol blend, Polym. Degrad. Stab. 98 (2013) 2529–2536. doi:10.1016/j.polymdegradstab.2013.09.012.

[34] V. P. M., olga B. Nazarenko, Thermal degradation of polymer blends, composites and nanocomposites, in: P.M. Visakh, Y. Arao (Eds.), Therm. Degrad. Polym. Blends, Compos. Nanocomposites, Springer, Kyoto, Japan, 2015: pp. 1–16. https://books.google.ie/books?id=39C9BwAAQBAJ&pg=PA3&dq=caly+blend+in+polymer+reduce+thermal+resistance&hl=en&sa=X&ved=0ahUKEwjjxuKFydvVAhVnLMAKHXHvCb0Q6AEIJTAA#v=onepage&q=caly blend in polymer reduce thermal resistance&f=false (accessed August 16, 2017).

[35] H. Ismail, P. Pasbakhsh, M.N.A. Fauzi, A.A. Bakar, Morphological, thermal and tensile properties of halloysite nanotubes filled ethylene propylene diene monomer (EPDM) nanocomposites, Polym. Test. 27 (2008) 841–850. doi:10.1016/j.polymertesting.2008.06.007.

[36] P. Russo, S. Cammarano, E. Bilotti, T. Peijs, P. Cerruti, D. Acierno, Physical properties of poly lactic acid/clay nanocomposite films: Effect of filler content and annealing treatment, J. Appl. Polym. Sci. 131 (2014). doi:10.1002/app.39798.

[37] F.-D. Kopinke, M. Remmler, K. Mackenzie, M. Möder, O. Wachsen, Thermal decomposition of biodegradable polyesters—II. Poly(lactic acid), Polym. Degrad. Stab. 53 (1996) 329–342. doi:10.1016/0141-3910(96)00102-4.

[38] G. Perego, G.D. Cella, Mechanical Properties, in: R. Auras, L.T. Lim, S.E.M. Selke, H. Tsuji (Eds.), Poly(Lactic Acid) Synth. Struct. Prop. Process. Appl., NJ. USA: Wiley, 2010: pp. 141–154. http://onlinelibrary.wiley.com/book/10.1002/9780470649848

(accessed June 1, 2015).

[39] H.Y. Liu, L. Du, Y.T. Zhao, W.Q. Tian, In vitro hemocompatibility and cytotoxicity evaluation of halloysite nanotubes for biomedical application, J. Nanomater. 2015 (2015) 1–9. doi:10.1155/2015/685323.

[40] R. Piccolo, T. Pilgrim, How these stent design characteristics may affect PCI outcomes going forward. The Impact of Thin-Strut, Biodegradable Polymer Stent Designs, Card. Interv. Today. 11 (2017) 43–46. http://citoday.com/pdfs/cit0117_F3_Pilgrim.pdf (accessed August 17, 2017).

[41] J.M. Raquez, Y. Habibi, M. Murariu, P. Dubois, Polylactide (PLA)-based nanocomposites, Prog. Polym. Sci. 38 (2013) 1504–1542. doi:10.1016/j.progpolymsci.2013.05.014.

[42] Y. Lvov, A. Aerov, R. Fakhrullin, Clay nanotube encapsulation for functional biocomposites, Adv. Colloid Interface Sci. (2014). doi:10.1016/j.cis.2013.10.006.

[43] R. babu Valapa, P. G., V. Katiyar, Hydrolytic degradation behaviour of sucrose palmitate reinforced poly(lactic acid) nanocomposites, Int. J. Biol. Macromol. 89 (2016) 70–80. doi:10.1016/j.ijbiomac.2016.04.040.

[44] Y.-B. Luo, X.-L. Wang, Y.-Z. Wang, Effect of TiO2 nanoparticles on the long-term hydrolytic degradation behavior of PLA, Polym. Degrad. Stab. 97 (2012) 721–728. doi:10.1016/j.polymdegradstab.2012.02.011.

[45] M.-X. Li, S.-H. Kim, S.-W. Choi, K. Goda, W.-I. Lee, Effect of reinforcing particles on hydrolytic degradation behavior of poly (lactic acid) composites, Compos. Part B Eng. 96 (2016) 248–254. doi:10.1016/j.compositesb.2016.04.029.

[46] Y. Tokiwa, B.P. Calabia, C.U. Ugwu, S. Aiba, Biodegradability of plastics., Int. J. Mol. Sci. 10 (2009) 3722–42. doi:10.3390/ijms10093722.

[47] A.C. Vieira, J.C. Vieira, J.M. Ferra, F.D. Magalhães, R.M. Guedes, A.T. Marques, Mechanical study of PLA – PCL fibers during in vitro degradation, J. Mech. Behav. Biomed. Mater. (2011) 451–460. doi:10.1016/j.jmbbm.2010.12.006.

[48] M. Vert, After soft tissues, bone, drug delivery and packaging, PLA aims at blood, Eur. Polym. J. 68 (2015) 516–525. doi:10.1016/j.eurpolymj.2015.03.051.

[49] H.B. Jeon, D.H. Kang, J.H. Gu, S.A. Oh, J. Bergsma, W. de Bruijn, F. Rozema, J. Rubin, M. Yaremchuk, J. Orringer, V. Barcelona, S. Buchman, J. Wiltfang, H. Merten, S. Schultze-Mosgau, M. Imola, D. Hamlar, W. Shao, R. Mackool, J. Yim, J. McCarthy, Y. Katsuragi, A. Gomi, A. Sunaga, A. Xue, J. Koshy, W. Weathers, R. Bell, C. Kindsfater, W. Pietrzak, D. Sarver, M. Verstynen, B. Eppley, L. Morales, R. Wood, H. Kwon, S. Kim, S. Jung, A. Kumar, D. Staffenberg, J. Petronio, E. Bergsma, F. Rozema, R. Bos, R. Miller, J. Brady, D. Cutright, R. Laughlin, M. Block, R. Wilk, E. Rha, H. Paik, J. Byeon, N. Sevastjanova, L. Mansurova, L. Dombrovska, Delayed Foreign Body Reaction Caused by Bioabsorbable Plates Used for Maxillofacial Fractures, Arch. Plast. Surg. 43 (2016) 40. doi:10.5999/aps.2016.43.1.40.

[50] Y. Marois, Z. Zhang, M. Vert, X. Deng, R.W. Lenz, R. Guidoin, Bacterial Polyesters for biomedical applications: In vitro and invivo assessments of sterization, degradation rate and biocompatibility of poly (2-gydroxyoctaanoate) (PHO), in: C.M. Agrawal, J.E. Parr, S.T. Lin (Eds.), Synth. Bioabsorbable Polym. Implant. Issue 1396, ASTM International, 2000: pp. 12–38. https://books.google.com/books?id=WcdolvJg-1MC&pgis=1 (accessed December 17, 2015).

[51] M. Murariu, A.-L. Dechief, R. Ramy-Ratiarison, Y. Paint, J.-M. Raquez, P. Dubois, Recent advances in production of poly(lactic acid) (PLA) nanocomposites: a versatile method to tune crystallization properties of PLA, Nanocomposites. 1 (2015) 71–82.

[52] J.W. (Joe W.. McPherson, Accelerated degradation, in: J.W. (Joe W.. McPherson (Ed.), Reliab. Phys. Eng. Time-to-Failure Model., 2nd ed., Springer, 2013: pp. 91–104. https://books.google.ie/books?id=LWRHAAAAQBAJ&pg=PA91&lpg=PA91&dq=degradation+process+shorten+with+elevated+temperature&source=bl&ots=-RdYcpMESR&sig=O3wTNI7BppLXnILXF8Gj3NcTX9A&hl=en&sa=X&ved=0ahUKEwjildvikefYAhUjDcAKHRRGCIYQ6AEILDAA#v=onepage&q=degradati (accessed January 20, 2018).